Journal of Pharmaceutical Sciences 106 (2017) 1952-1960

Contents lists available at ScienceDirect

Journal of Pharmaceutical Sciences

journal homepage: www.jpharmsci.org

Pharmaceutical Biotechnology

Characterization of Protein Particles in Therapeutic Formulations Using Imaging Flow Cytometry

Christine Probst [1,*], Yuanchun Zeng [2], Rong-Rong Zhu [2]

[1] Amnis, a part of MilliporeSigma, Seattle, Washington 98119
[2] MilliporeSigma Corporation, Bedford, Massachusetts 01730

ARTICLE INFO

Article history:
Received 28 February 2017
Revised 12 April 2017
Accepted 17 April 2017
Available online 27 April 2017

Keywords:
biopharmaceuticals characterization
imaging methods
light scattering
physical characterization
protein aggregation
protein formulation

ABSTRACT

Quantitation of particles >10 μm in therapeutic protein formulations is required by pharmacopeia guidelines, and characterization of particles <10 μm is increasingly expected. Established methods offer limited ability to detect or characterize small particles; consequently, new methods are needed to measure the sub-10 μm size range. Here, we evaluate imaging flow cytometry (IFC) as a new method for detection of protein aggregates, taking advantage of key enabling attributes including rapid multi-modal high-resolution imaging of individual particles, low sample volume, high sampling efficiency, wide dynamic size and concentration range, and low clog risk. IFC sensitivity was compared with dynamic imaging, a "gold standard" technique for analysis of particles in protein formulations. Both techniques yielded similar results for polystyrene beads ≥2 μm. However, IFC demonstrated greater protein particle detection sensitivity, especially for the sub-10 μm size range. Interestingly, for an aggregated lysozyme sample, IFC detected protein particles using fluorescence images, whereas dynamic imaging failed to detect even large particles >25 μm due to high transparency. The results corroborate implementation of IFC as an advanced technique for protein particle analysis, offering in-depth characterization of particle physical and chemical properties, and enhanced sensitivity for sub-10 μm and transparent particles.

Introduction

Therapeutic proteins have greatly advanced treatment for a wide range of human medical conditions including cancer, infection, and autoimmune disease.[1,2] However, individual protein molecules are susceptible to aggregation, especially at high concentrations used in pharmaceutical formulations.[3] Protein aggregates pose numerous safety concerns, including lowered effective dose, blood vessel occlusion, and immunogenicity.[4-7] Furthermore, additional contaminant species including silicone oil droplets, air bubbles, fibers, and glass and metal particles uniquely impact formulation stability and safety.[8-10] Consequently, United States and European regulatory agencies have set concentration limits for particles >10 μm, increasingly expect analysis of particles in the 0.1-10 μm size range, and have emphasized the importance of characterization of particle type in protein therapeutics.[11]

Light obscuration remains the designated method for formulation lot release by pharmacopeia guideline USP <787>, despite being a non-characterization method offering limited sensitivity to protein particles, which are transparent in nature. Another limitation of light obscuration is the potential need to dilute samples to accommodate a large minimum sample volume and low concentration dynamic range, which may impact the measurement through reversal of concentration-dependent species.[12] To supplement light obscuration, dynamic imaging (DI) has been rapidly adopted based on greater sensitivity, lower sample volume requirements, and larger concentration dynamic range.[13-15] DI collects brightfield imagery of particles passing through a flow cell, allowing direct measurement of particle size and determination of particle type through image analysis.[16] Nevertheless, both methods use light transmission for detection of particles in relatively large sample volumes, potentially missing transparent particles such as protein aggregates and distorting states of concentration-dependent species.[17,18] Therefore, a truly orthogonal method is needed to satisfy increasing demands for comprehensive characterization of particles in therapeutic formulations.[19]

Conflicts of interest: The authors are current or former employees of MilliporeSigma, manufacturer of Amnis imaging flow cytometers.
This article contains supplementary material available from the authors by request or via the Internet at http://dx.doi.org/10.1016/j.xphs.2017.04.034.

* *Correspondence to:* Christine Probst (Telephone: +1-714-686-4081; Fax: +1-206-576-6895).
E-mail address: christine.probst@emdmillipore.com (C. Probst).

http://dx.doi.org/10.1016/j.xphs.2017.04.034
0022-3549/

Imaging flow cytometry (IFC) is one potentially powerful orthogonal method for analysis of therapeutic formulations. IFC shares commonalities with DI, with both platforms collecting single-particle image data at high throughput. In contrast to DI, IFC is capable of simultaneous brightfield, side-scatter, and multi-channel fluorescence imaging, enabling the use of fluorescent probes specific for the different components in the sample and additional analysis of particle refractive index from scattered light. Additionally, IFC requires low sample volumes (as small as 20 μL) and measures a large concentration range (up to 10^9/mL), negating the need for sample dilution. Compared to DI, IFC uses higher magnification objectives to achieve greater image resolution, maintaining 100% sampling efficiency using hydrodynamic sheath focusing. IFC has been extensively developed for a wide array of cell-based assays and recently applied for analysis of small particles in the micron to sub-micron ranges[20-22]; however, its potential for analysis of protein formulations has not yet been evaluated.

Given the conceptual advantages of IFC for analysis of protein therapeutics, the goal of this study is to evaluate the sensitivity and characterization capability of IFC in comparison to DI. Monodisperse polystyrene beads were used for initial assessment of both platforms, and stressed IgG and lysozyme were used as models for aggregated protein. To leverage the fluorescence imaging capabilities of IFC, protein particles were stained using the ProteoStat fluorescent dye, a "mix and read" dye which enhances fluorescent intensity upon binding protein aggregates. All samples were obtained from commercial vendors to allow reproduction of results.

Materials and Methods

IFC experiments were performed using a 12-channel ImageStream$^{®X}$ Mark II (MilliporeSigma, Seattle, WA); DI experiments were performed using a FlowCam® VS series (Fluid Imaging Technologies, Scarborough, ME). Calcium-free, magnesium-free, phosphate buffered saline was purchased from Invitrogen (Carlsbad, CA) and used as IFC sheath. Polystyrene standards (4.4 and 10.2 μm) were purchased from Bangs Laboratories (Fishers, IN). FluoSphere fluorescent polystyrene standards (1 and 2 μm) were purchased from Invitrogen. Enzo ProteoStat® Protein Aggregation Standards containing stressed and unstressed IgG and ProteoStat Protein Aggregation Assay containing ProteoStat staining reagents and stressed and unstressed lysozyme were purchased from Enzo Life Sciences (Farmingdale, NY). ProteoStat staining reagent is provided at 3 mM ("1000X") stock concentration. BODIPY® 493/503 and SYTO® 62 Red Fluorescent Nucleic Acid Stain were purchased from Thermo Fisher Scientific (Waltham, MA).

Sample Preparation

Polystyrene beads were prepared to approximately 1×10^6 particles/mL based on concentration values provided by the manufacturer. Lysozyme and IgG proteins were stressed by thermal denaturation by the manufacturer using a proprietary protocol. Stressed and unstressed proteins were supplied in lyophilized form and reconstituted with nuclease-free water (IgG: 73 μg/mL; lysozyme: 50 μg/mL). For DI experiments, polystyrene beads were diluted 10X to avoid coincidence. Protein samples were fluorescently labeled by mixing with an equal volume of staining cocktail containing 1.5 μM BODIPY, 1.25 μM SYTO 62, and 0.375 μM ProteoStat in 1X ProteoStat assay buffer and incubating for at least 15 min prior to image acquisition. Silicone oil droplets and bacteria represent 2 other major contaminants that might be mistakenly counted as protein aggregates. To differentiate between these contaminants, the lipophilic dye BODIPY was added to label silicone oil droplets,[23] and RNA-specific dye SYTO was used to label bacteria. However, as experimental samples evaluated in this manuscript were presumed not to contain silicone oil droplets or bacteria, sample characterization using BODIPY and SYTO dyes was not performed. To assess the potential impact of the fluorescent labeling protocol on protein aggregation and particle concentration, unlabeled samples were prepared and particle counts were compared to labeled samples using DI. All concentrations reported are corrected for dilution factors.

IFC Measurement

IFC experiments were conducted using a 40X magnification objective in high-sensitivity mode (flow rate 1.14 μL/min) which generates images with 0.5 μm pixel resolution and a 60-μm wide field-of-view. Brightfield was set to channels 1 (emission 457/45 nm) and 9 (emission 582/25); side-scatter to channel 12 (emission 762/35); fluorescent bead images were collected in channel 2 (528/65); and ProteoStat dye images were collected in channel 4 (610/30). For polystyrene bead experiments, the 785-nm side-scatter excitation laser was set to 1 mW; for protein experiments, 20 mW. For fluorescent bead experiments, the 488-nm fluorescence excitation laser was set to 1 mW; for protein experiments, 200 mW. A total of 35 μL of the sample was loaded into the instrument, and 20 μL was primed out before collecting the remaining 15 μL. SpeedBead calibration particles were used for instrument autofocusing during sample acquisition, and excluded from data using characteristic high scatter and low brightfield area or fluorescence. To evaluate instrument operation without SpeedBeads, the SpeedBead container was replaced with deionized water and experiments evaluating protein particles were repeated.

Analysis of IFC Data

Analysis of IFC data was performed in IDEAS® 6.2 (MilliporeSigma) image analysis software. Images were compensated for spectral spillover from fluorescence dyes using single-color compensation controls so that each channel measured only fluorescence, brightfield, or side-scatter. Object detection was performed using the LevelSet mask applied to the brightfield image, except for lysozyme samples where it was applied to the ProteoStat image due to particle transparency in brightfield. Particle size was measured using the *Diameter* feature, which measures the diameter of a circle that occupies the same area of the object in microns. Total particle intensity was measured using the *Intensity* feature, which calculates the sum of background-subtracted intensities for each pixel. Average pixel intensity was calculated using the *Mean Pixel* feature, which divides *Intensity* by the number of pixels. Particle shape was evaluated using the *Aspect Ratio* feature, which divides the length of the minor axis by the length of the major axis. Particle transparency was measured using the *Contrast* feature, which detects large changes of pixel values in the image by measuring the pixel intensities in the 3×3 block around each pixel. Absolute particle concentration was measured using the *Obj/mL* feature, which divides the number of particles measured by the volume analyzed.

DI Measurement

DI experiments were performed using a 10X magnification objective and a 100 μm flow cell. A total of 1.0 mL of the sample was loaded into the instrument and 0.5 mL was collected using a flow rate of 0.2 mL/min. Autoimage was set to 17 frames/s resulting in a sampling efficiency of 17.3%. Both light and dark pixels were used for thresholding. Images were captured using a close holes value of 2, and distance to nearest neighbor of 3 using a 0 μm threshold.

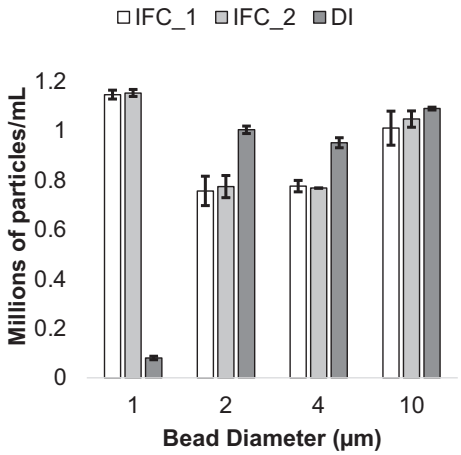

Figure 1. Particle concentration measured with IFC (40X) or DI (10X) for 1-10 μm polystyrene bead standards. Beads 2 μm and below are fluorescent. Each data point represents the average of 2 datasets for IFC and 3 datasets for DI. IFC measurements were collected on 2 separate instruments (IFC_1, IFC_2) to assess reproducibility. Error bars represent 1 SD between separate datasets.

DI Analysis

Analysis of DI data was performed using Visual Spreadsheet (FluidImaging) image analysis software. Concentration was measured in *Obj/mL*, particle size was measured using *Equivalent Circular Diameter*. Representative imagery was extracted using Lumetics software.

Results

Measurement of Polystyrene Standards Using IFC and DI

The sensitivity of IFC was compared with DI using polystyrene standards ranging from 1 to 10 μm. The ImageStream^X Mark II uses SpeedBeads, 1 μm non-fluorescent carboxylated polystyrene beads, as an internal calibration for instrument autofocusing. SpeedBeads are present in high concentrations (1.6×10^7/mL) during a sample run, and consequently must be removed during acquisition or analysis so that only particles originating from the sample are measured. SpeedBeads can be excluded from sample particles using their characteristically small area, high side-scatter, or non-fluorescence. Polystyrene standards 4 μm and above could be discriminated from SpeedBeads based on higher side-scatter, whereas polystyrene beads 2 μm and below were fluorescent, allowing discrimination from SpeedBeads using a fluorescence threshold. Comparable particle counts were obtained with both IFC and DI for standards above 2 μm in size; however, IFC detected 14.4-fold more particles compared to DI for the 1 μm standard (Fig. 1). Concentration measurements were repeated on 2 IFC instruments, demonstrating reproducibility of the results.

Accurate characterization of particle morphology by microscopy is determined by image resolution and quality, with higher resolution techniques allowing characterization of increasingly smaller particles. Figure 2 compares brightfield image quality of 1-10 μm polystyrene beads for IFC collected using a 40X magnification objective versus DI collected using a 10X magnification objective. As expected from the higher magnification, IFC produces higher quality images compared to DI. Some images are slightly out of focus with IFC and show a black core, due to the bead falling outside the focal plane of the objective, which is 4 μm at 40X.

Both IFC and DI provide direct particle size measurements by converting the number of pixels within an image into a physical area in square microns. Measuring particle size requires "object detection" to discriminate particle-containing pixels from particle-free pixels, a process known as "thresholding" using DI and "masking" using IFC. Particle sizing with IFC was compared with DI using polystyrene bead standards 1-10 μm. Particle thresholding was performed using both light-and-dark pixels with DI and the LevelSet mask with IFC based on its tight fit around the particle boundary upon visual inspection. All bead sizes were clearly visible

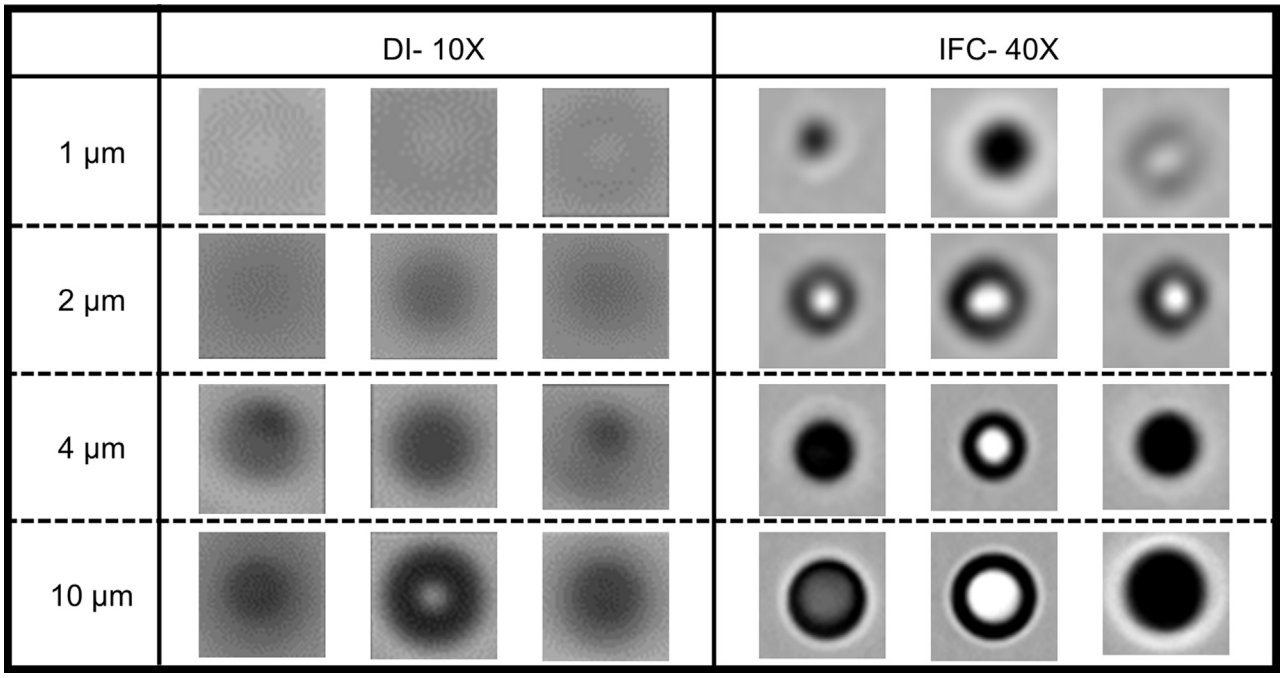

Figure 2. Representative imagery of 1-10 μm polystyrene beads measured with DI collected at 10X magnification or IFC collected at 40X magnification.

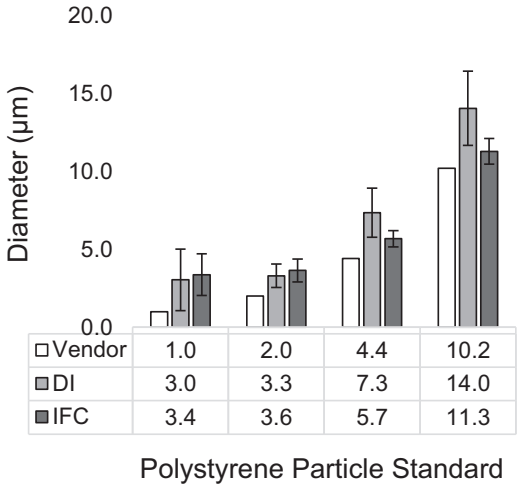

Figure 3. Mean particle brightfield *Diameter* measured with IFC or DI for 1-10 µm polystyrene beads. Beads 2 µm and below are fluorescent to allow discrimination from SpeedBeads. Error bars represent 1 SD within an individual dataset.

in the brightfield channel with IFC and consequently, masking was performed using the brightfield channel as the input. Figure 3 shows that particle sizes measured with both methods correlate well with known bead diameters, although both methods overestimate particle size and have substantial error bars due to the limited pixel resolution of collected imagery and presence of out-of-focus particles.

Quantitation of IgG and Lysozyme Particles With IFC and DI

Stressed and unstressed IgG and lysozyme were obtained from a commercial vendor. To leverage the fluorescence imaging capabilities of IFC, all samples (including samples for DI experiments) were labeled with ProteoStat, a no-wash dye featuring minimal fluorescence in the presence of monomeric protein and a 20-90-fold fluorescence enhancement upon binding aggregated protein.

Several control studies were performed to evaluate an impact of fluorescence labeling on the results. Figure 4 shows bivariate plots for brightfield *Diameter* versus ProteoStat *Intensity* for controls and aggregated protein samples measured with IFC. The fluorescent label itself has the potential to impact sample properties, either through formation of dye precipitates or aggregation or disaggregation of sample particles. Comparison of unlabeled deionized water (Fig. 4a) with fluorescently labeled deionized water (Fig. 4b) demonstrates that fluorescent labeling forms dye particles with ProteoStat *Intensity* as high as 25,000. Note that SpeedBeads were not used during collection of the unlabeled filtered water sample (Fig. 4a), as SpeedBeads were excluded from acquisition for dye labeled samples (Figs. 4b-4f) using fluorescence versus side-scatter intensity, which was not possible for the unlabeled sample. Although no fluorescence dyes were added to the unlabeled deionized water sample, 2.96×10^6 particles/mL were detected by brightfield or side-scatter, which we attributed to a combination of high camera sensitivity and particle carryover from instrument buffers and fluidic lines. The size distribution of these particles was small, with 99.7% below 10 µm. To obtain a clean signal, dye precipitates and other non-fluorescent particles smaller than 10 µm were considered background and removed using a threshold of 25,000 for ProteoStat *Intensity* and 10 for *Diameter*. Note that with this approach, particles smaller than 10 µm will still be counted if ProteoStat *Intensity* is above 25,000. To evaluate the possibility that fluorescence labeling induced protein aggregation, unstressed and stressed protein samples at the same concentration were measured (Figs. 4c-4f). Few particles were measured in the unstressed sample compared to the stressed sample, suggesting that fluorescent labeling does not cause aggregation of monomeric protein.

To further examine the effect of dye labeling on particle properties, fluorescently labeled and unlabeled samples were compared using DI (Supplementary Table S1). Similar size distributions were measured for labeled and unlabeled IgG and lysozyme particles; however, IgG particle concentration decreased by 20% and lysozyme particle concentration decreased by 53% (though few lysozyme particles were detected by DI in either condition). The decrease in particles measured may be attributed to aggregation reversal following the 2-fold sample dilution upon fluorescent labeling, or changes in background illumination due to the presence of fluorescence dyes excitable by brightfield illumination. Nonetheless, the results indicate that the fluorescent labeling protocol does not appear to substantially induce aggregation or disaggregation.

SpeedBeads used for autofocusing may also affect particle counts by forming complexes with protein aggregates, or even acting as vehicle for protein agglomeration. Although this was not directly evaluated, we note that SpeedBeads are not required for IFC operation, which was demonstrated by replacing the SpeedBead container with deionized water and repeating the experiment with comparable results (Supplementary Fig. S1).

Particle concentrations measured with DI and IFC were compared to evaluate the sensitivity of each method to protein aggregates. Figure 5 shows particle concentration measured for unstressed and stressed IgG particles for 2-10, 10-25, and >25 µm ranges. Overall trends match between IFC and DI, with the stressed IgG sample containing more particles compared to the unstressed IgG sample. However, absolute counts are much higher with IFC compared to DI, especially for the smaller sizes, where IFC measured an 80-fold higher concentration for particles 2-10 µm, and a 14-fold higher concentration for particles 10-25 µm (Table 1). Figure 6 shows particle concentrations for unstressed and stressed lysozyme particles. In this case, trends between IFC and DI do not match, with IFC measuring an 11-fold increase in particle concentration for the stressed sample compared to the unstressed sample, but DI measuring a 25% decrease. Interestingly, this discrepancy cannot only be attributed to increased IFC sensitivity to small particles, as IFC detected 2.9×10^5 particles/mL >10 µm and 2.2×10^4 particles/mL >25 µm, while DI measured 0 particles/mL >10 µm (Table 1).

Multi-Modal Characterization of Particles With IFC

To understand why trends between DI and IFC did not agree for the lysozyme samples, the particle physical and chemical properties were evaluated using multi-modal IFC data. Figure 7 shows representative brightfield, side-scatter, and fluorescence imagery for the largest particles measured, and quantitative feature values for particles 10-25 µm. *Aspect Ratio* was used to characterize particle shape, and similar measurements for IgG (0.61 ± 0.18) and lysozyme (0.65 ± 0.20) particles indicate similar elongated morphology. Brightfield *Contrast* values were lower for lysozyme particles (0.21 ± 0.21) compared to IgG particles (3.43 ± 2.17). Inspection of brightfield imagery reveals that the low lysozyme contrast is due to the high transparency of these particles, resulting in similar pixel intensity within the lysozyme particles compared to the image background. Side-scatter *Mean Pixel* was much lower for lysozyme particles (9 ± 120) compared to IgG (266 ± 157), indicating lysozyme particles have low refractive index. Taken together, these results indicate that the lysozyme particles do not strongly interact with light through absorption or

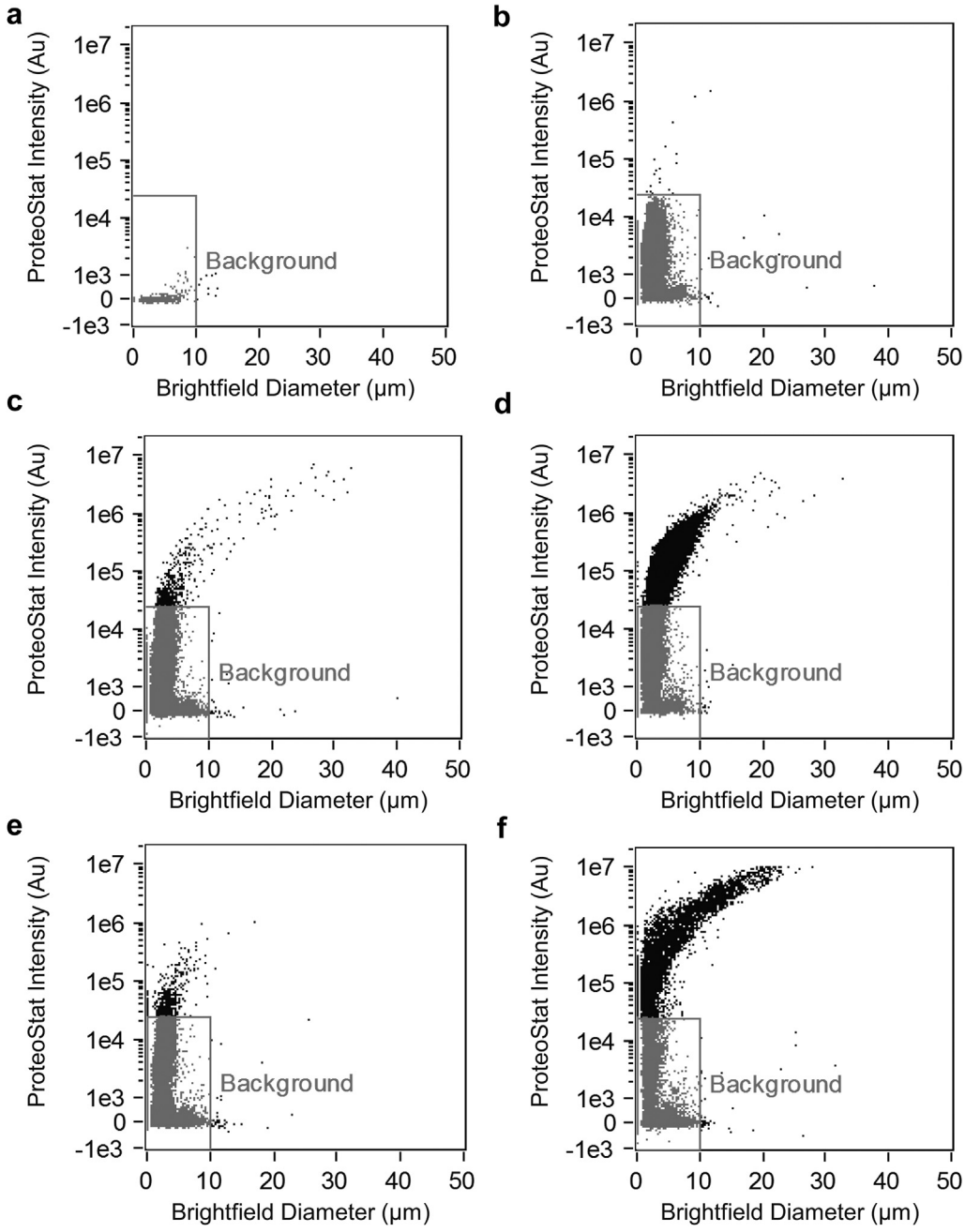

Figure 4. Bivariate plots collected with IFC showing brightfield *Diameter* measured in μm versus ProteoStat *Intensity* measured in arbitrary units (Au) for unlabeled filtered water (a), fluorescently labeled filtered water (b), unstressed IgG (c), stressed IgG (d), unstressed lysozyme (e), and stressed lysozyme (f).

scattering, explaining why these particles are difficult to detect with light-based DI methods. On the other hand, ProteoStat *Mean Pixel* was high for both lysozyme (2919 ± 713) and IgG (2091 ± 893), rendering them easily detectable in the fluorescence channel collected with IFC. Note that high side-scatter *Mean Pixel* standard deviations measured for lysozyme particles are due to attachment of SpeedBeads, seen as bright spots in the side-scatter channel, which are negatively charged and likely adsorbed via electrostatic interactions to positively charged lysozyme (isoelectric point of 11.35). The same experiment was repeated without SpeedBeads, resulting in no observed bright spots in the side-scatter channel and lower standard deviations for side-scatter *Mean Pixel* (11 ± 33) for lysozyme particles (Supplementary Fig. S2).

Discussion

Sensitivity and Dynamic Range

Industry regulations are increasingly emphasizing characterization of sub-10 μm particles in protein formulations in addition to particles 10 μm and larger. Current analytical methods typically measure a subset of this size range, requiring multiple techniques to evaluate the full 0.1-100 μm size range of interest. As an example, scatter-based nanoparticle tracking analysis may be used to characterize particles 0.1-1 μm, while light transmission-based DI may be used to characterize particles 1-100 μm. IFC, in contrast, is capable of measuring a wide dynamic size range through simultaneous collection of light transmission (brightfield), fluorescence,

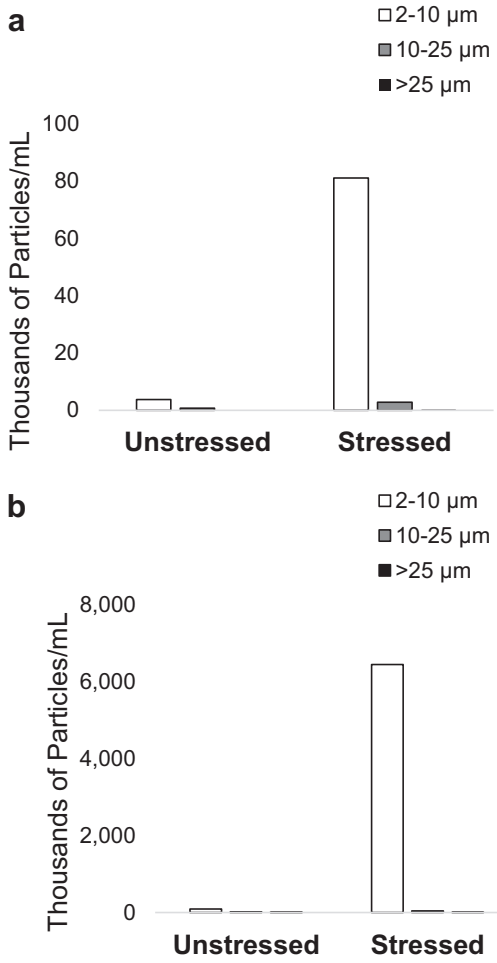

Figure 5. Particle concentration for unstressed and thermally stressed IgG measured with DI (a) and IFC (b).

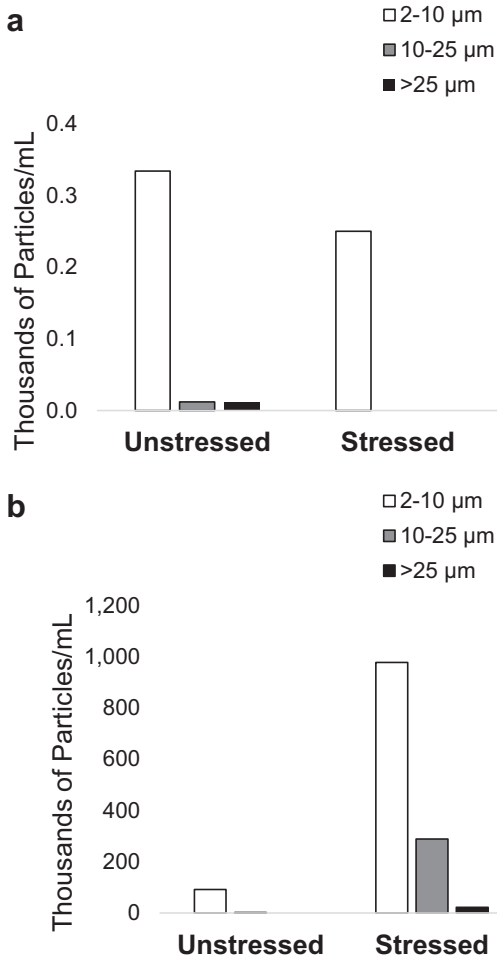

Figure 6. Particle concentration for unstressed and thermally stressed lysozyme measured with DI (a) and IFC (b).

and side-scatter images. Side-scatter and fluorescence are more sensitive to small particles compared to brightfield and allow detection in the sub-micron range. Previous studies in biological microparticle analysis have demonstrated that scatter and fluorescence channels of IFC provide sensitive detection of 50-nm fluorescent beads and 200-nm liposomes.[21,22] The maximum size of particles detectable by IFC is determined by the field of view of the objective lens used, which is 60 µm wide and 450 µm long with the 40X objective, and can be expanded to 120 × 900 µm using the 20X objective.

In this study, the sensitivity of IFC was compared to DI using polystyrene bead standards and aggregated protein samples. Although IFC and DI measured similar concentrations for polystyrene standards 2 µm and up (matching the 2 µm lower size limit reported by the DI manufacturer), IFC measured 14.4-fold higher concentrations for 1 µm fluorescent polystyrene standards.

Table 1
Fold Increase in Particle Concentration Measured With IFC Compared to DI

Sample Type	Particle Size (µm)	Particle Concentration (#/mL)		Fold Increase
		DI	IFC	IFC/DI
Polystyrene beads	1	79,839	1,146,018	14.4
	2	1,003,876	755,951	0.75
	4	950,943	775,657	0.82
	10	1,089,515	1,010,453	0.93
H_2O	2-10	0	2464	N/A
	10-25	0	2312	N/A
	>25	0	154	N/A
Stressed IgG	2-10	81,070	6,452,652	79.59
	10-25	2846	40,332	14.2
	>25	290	547	1.9
Stressed lysozyme	2-10	250	977,484	3910
	10-25	0	288,387	N/A
	>25	0	21,669	N/A

A fold increase of "N/A" (not applicable) indicates division by 0.

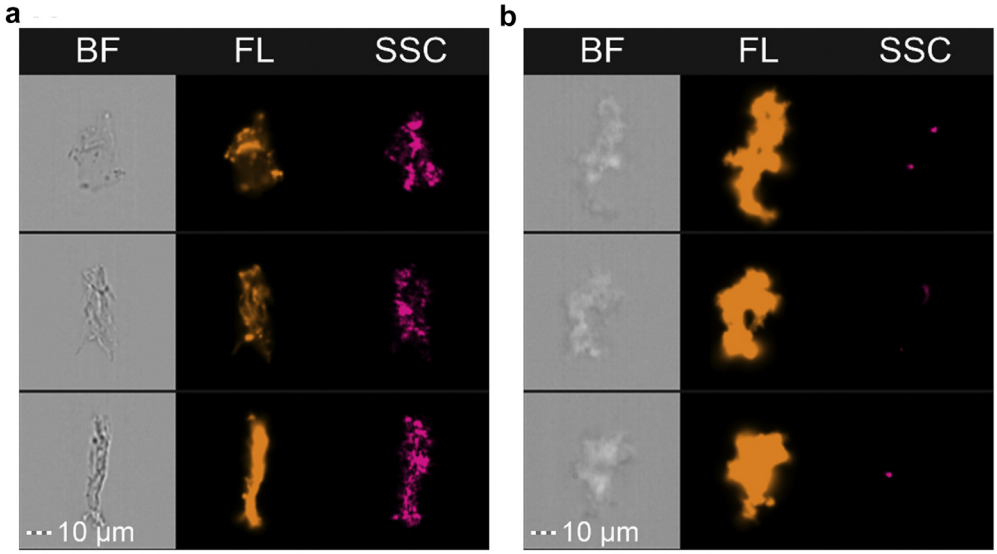

	a	b
BF Aspect Ratio	0.61 ± 0.18	0.65 ± 0.20
BF Contrast	3.43 ± 2.17	0.21 ± 0.21
FL Mean Pixel Intensity	2,091 ± 893	2,919 ± 713
SSC Mean Pixel Intensity	266 ± 157	9 ± 120

Figure 7. Representative multi-modal imagery and quantitative feature values of protein particles measured with IFC. Brightfield (BF), ProteoStat fluorescence (FL), and side-scatter (SSC) imagery of thermally stressed IgG particles (a) and thermally stressed lysozyme particles (b). Image feature mean values ± standard deviations are shown for the 10-25 µm population for each particle type.

Superior detection capacity of IFC was particularly evident with samples containing protein particles known to have lower refractive index compared to polystyrene beads. IFC measured 77.1-fold higher particles for a stressed IgG sample and 5.15×10^3-fold higher particles for a stressed lysozyme sample, which was essentially undetectable with DI despite the presence of large particles (>25 µm). Inspection of multi-modal IFC data attributed the lack of lysozyme particle detection with DI to the high transparency and low light-scattering by these particles (Fig. 7), emphasizing the utility of fluorescence-based detection of protein aggregates (via staining with extrinsic dyes) as an important complementary technique for characterization of therapeutic formulations.

Image Resolution, Sampling Efficiency, and Clogging

Characterization of particle type within protein formulations is necessary to evaluate formulation safety and predict future particle formation. Imaging-based methods including DI and IFC provide the opportunity to automatically identify particles using morphological attributes via image filtering.[16] Accurate classification of particles with image filtering requires a minimum image resolution, or number of pixels, which is directly related to particle size and magnification of the analytical method. In microscopy, magnification power is inversely related to depth of field, the distance in the axial direction when images are in focus. When imaging in flow, particles passing through the flow cell but not within the depth of field of the objective are out of focus or not imaged, thus creating a tradeoff between sampling efficiency, magnification, and image resolution. Sampling efficiency may be improved using increasingly narrow flow cells; however, this approach increases the likelihood of instrument clogging and sample loss. Leading DI instruments (Micro-Flow Imaging, FlowCam) use low to mid-range magnification objectives and interchangeable flow cell diameters to optimize for sampling efficiency and clog risk.[24] IFC overcomes these limitations by hydrodynamically focusing particles into a narrow core stream using sheath fluid. IFC can be equipped with up to a 60X objective (0.33 µm pixel resolution), maintains 100% sampling efficiency, and has low clog risk due to a fixed 250 µm flow cell. Hydrodynamic sheath focusing employed by IFC allows measurement of higher particles concentrations compared to DI by aligning them to a narrow core stream, mitigating the need for sample dilution which may potentially reverse aggregate formation. Therefore, IFC may prove a useful tool for analysis of concentration-dependent aggregation at true formulation conditions.

Figure 2 shows that IFC produces qualitatively higher image resolution compared to DI for polystyrene beads 1-10 µm using typical instrument settings (DI 10X; IFC 40X). Particle sizing accuracy for IFC and DI was evaluated by comparing measured diameter to those reported by the manufacturer. IFC and DI produced similar size measurements but slightly overestimated bead size compared to manufacturer measurements (Fig. 3). These results indicate that IFC provides accurate size measurements and may improve morphology-based characterization of smaller particles compared to DI based on higher image resolution.

Multi-Modal Particle Characterization

The capability of IFC to simultaneously collect brightfield, side-scatter, and fluorescence imagery represents a key distinguishing feature that enables in-depth characterization of the particle physical and chemical properties. Brightfield imagery provides particle shape and size measurements; side-scatter may be used to measure particle granularity and refractive index; and fluorescence

imaging provides the unique opportunity to detect particles, identify particles, or evaluate particle chemical properties.[25] As an example, fluorescence probes have been used to measure protein aggregates by fluorescence microscopy[26,27] and flow cytometry.[23,28,29] Although fluorescence microscopy provides similar data to IFC, it is limited by low sample volumes[26] or the need for membrane filtration which may affect sample properties. Additionally, fluorescence microscopy often requires manual image acquisition and analysis, which is time consuming and potentially subjective. Although flow cytometry remains a powerful high throughput technique for measuring protein particles, lack of imagery prevents direct sizing of protein particles; consequently, scatter measurements are used to estimate particle size. Conversion of scatter measured in arbitrary units to particle diameter in microns has relied on bead calibration standards, which is known to underestimate particle size due to higher refractive index of beads compared to protein particles.[30,31] Another challenge is that the refractive index properties of protein aggregates vary widely depending on protein type and aggregation mechanism, as shown by higher scattering and contrast of IgG particles compared to lysozyme particles (Fig. 7).

ProteoStat was used to measure protein aggregation based on lack of covalent conjugation step, lack of a wash step, brighter signal compared to conventional extrinsic dyes (e.g., Thioflavin T), and compatibility with a wider range of proteins, surfactant, excipient, and pH conditions (ProteoStat protein aggregation assay user manual). ProteoStat undergoes a fluorescence enhancement upon binding the cross-beta quaternary structure of protein aggregates, allowing protein aggregation to be measured rather than particle unfolding.[32] Additional fluorescent dyes including Bis-ANS, Thioflavin T, and Nile Red may also be used to measure protein aggregation with IFC, which can be equipped with excitation lasers ranging from 375 to 642 nm, and can simultaneously measure 12 emission channels ranging from 430 to 800 nm.[25] Measurement of an individual dye or multiplexed analysis of several dyes using IFC may provide new insights into the connection between particle composition and potential immunogenicity.

IFC Limitations and Author Comments

Although IFC offers a number of advantages for analysis of therapeutic protein formulations, the technique also faces some limitations. One limitation of IFC is the lower volumetric flow rate compared to DI, as sample is processed at 1-4 μL/min depending on instrument settings. This limitation is mitigated in part by the greater sensitivity of IFC, which results in higher particle concentrations, especially in the sub-10 μm size range, allowing statistically robust measurements from a smaller sample volume. Consequently, IFC achieves similar sample throughput to MFI, allowing measurement of approximately 10 samples/h for typical sample volumes of 5-10 μL. However, this method is not well suited for measurement of very dilute particles, which typically include the largest particles in protein formulations. Thus, higher volumetric throughput techniques such as DI or light obscuration remain essential complementary methods for characterization of large and rare particles.

IFC achieves higher image resolution and wider concentration dynamic range compared to DI using hydrodynamic sheath focusing. However, sheath fluid has the potential to affect sample properties, particularly if the formulation is not stable in the sheath fluid used. The manufacturer recommended sheath for IFC is phosphate buffered saline due to historical application for cellular assays, although water may also be used, as well as formulation buffer if validated by the user. Although sheath fluid does not mix with the sample once a stable sample core is formed, there is some mixing for the first portion of the sample upon loading, diluting the sample. To reduce the effects of sheath mixing and dilution, the first 20 μL of the sample was purged upon sample loading, allowing IFC to produce accurate concentration measurements that matched DI (Fig. 1).

Another valid concern is that SpeedBeads, internal 1 μm polystyrene calibration particles used for autofocusing, may affect the analysis by acting as a resin for protein monomers or particles. IFC was originally developed for cellular assays; consequently, SpeedBeads are carboxylated to minimize interactions with negatively charged cell membranes through electrostatic repulsion. In this study, samples were collected both with and without SpeedBeads such that data quality could be evaluated in their presence or absence. Incorporation of fluorescence dyes specific to proteins or other particles of interest facilitates removal of SpeedBeads which are non-fluorescent. For protein experiments, the majority of SpeedBeads were removed during data analysis based on high side-scatter and lack of fluorescence. However, high-scattering and non-fluorescent objects such as metal particles or salt precipitates, which may potentially be of interest, will also be removed with SpeedBeads using this approach. SpeedBead interaction with sample particles is also possible, as seen by attachment to lysozyme particles triggered by electrostatic interactions (Fig. 7), resulting in inaccurate refractive index measurements. Due to potential issues introduced by SpeedBeads for analysis of protein formulations, the authors recommend operating the instrument without SpeedBeads. Repeating the experiments without SpeedBeads produced similar data (Supplementary Fig. S1) with high image quality (Supplementary Fig. S2), demonstrating that SpeedBeads are not necessarily required for instrument focusing.

One final observation is that the protein concentrations used in this study are much lower compared to typical pharmaceutical formulations. Proteins were diluted to 50-73 μg/mL from lyophilized powder to generate sufficient sample volumes for IFC and DI experiments. Therefore, the question remains whether IFC represents a suitable technique for pharmaceutical formulations which are typically prepared at much higher concentrations (tens to hundreds of mg/mL) in the presence of surfactant. Although data on high concentration formulations are yet to be published, it is our opinion based on IFC analysis of a large number of formulations on the market or in development (up to 200 mg/mL protein, up to 0.3% surfactant tested, data not shown) that typical pharmaceutical formulations can be successfully measured with no issues.

Conclusion

Industry regulations have been heightened for characterization of particles within therapeutic protein formulations, and characterization of the sub-10 μm size range is now expected. This study aimed to evaluate IFC as a new method for quantitation and characterization of sub-visible particles in protein formulations. Compared to established technique DI, IFC produced higher image resolution and provided more sensitive detection of protein aggregates when combined with fluorescence labeling, especially for sub-10 μm particles and even large transparent particles >25 μm. Additional benefits of IFC include low clog risk, small sample volume, and wide dynamic concentration range, allowing direct analysis of precious or concentrated samples. The results indicate that IFC may serve as a valuable orthogonal method for analysis of sub-visible particles within therapeutic formulations, in particular for evaluation of sub-10-μm particles, transparent particles, and concentration-dependent aggregates.

Acknowledgments

We thank Kristina Cunningham and Phil Morrissey for their support of this work, Chris Gillespie and Kevin Galipeau for assistance with experimental preparation, and Dave Thomas and Clark Merchant for providing access to Lumetics LINK™ software.

References

1. Leader B, Baca QJ, Golan DE. Protein therapeutics: a summary and pharmacological classification. *Nat Rev Drug Discov*. 2008;7:21-39.
2. Scott AM, Wolchok JD, Old LJ. Antibody therapy of cancer. *Nat Rev Cancer*. 2012;12:278-287.
3. Wang W, Singh SK, Li N, Toler MR, King KR, Nema S. Immunogenicity of protein aggregates—concerns and realities. *Int J Pharm*. 2012;431:1-11.
4. Carpenter JF, Randolph TW, Jiskoot W, et al. Overlooking subvisible particles in therapeutic protein products: gaps that may compromise product quality. *J Pharm Sci*. 2009;98:1201-1205.
5. Rosenberg AS. Effects of protein aggregates: an immunologic perspective. *AAPS J*. 2006;8:E501-E507.
6. Barnard JG, Babcock K, Carpenter JF. Characterization and quantitation of aggregates and particles in interferon-beta products: potential links between product quality attributes and immunogenicity. *J Pharm Sci*. 2013;102:915-928.
7. Kotarek J, Stuart C, De Paoli SH, et al. Subvisible particle content, formulation, and dose of an erythropoietin peptide mimetic product are associated with severe adverse postmarketing events. *J Pharm Sci*. 2016;105:1023-1027.
8. Gerhardt A, McGraw NR, Schwartz DK, Bee JS, Carpenter JF, Randolph TW. Protein aggregation and particle formation in prefilled glass syringes. *J Pharm Sci*. 2014;103:1601-1612.
9. Jones LS, Kaufmann A, Middaugh CR. Silicone oil induced aggregation of proteins. *J Pharm Sci*. 2005;94:918-927.
10. Tyagi AK, Randolph TW, Dong A, Maloney KM, Hitscherich Jr C, Carpenter JF. IgG particle formation during filling pump operation: a case study of heterogeneous nucleation on stainless steel nanoparticles. *J Pharm Sci*. 2009;98:94-104.
11. Weinbuch D, Zolls S, Wiggenhorn M, et al. Micro-flow imaging and resonant mass measurement (Archimedes)—complementary methods to quantitatively differentiate protein particles and silicone oil droplets. *J Pharm Sci*. 2013;102:2152-2165.
12. Shire SJ, Shahrokh Z, Liu J. Challenges in the development of high protein concentration formulations. *J Pharm Sci*. 2004;93:1390-1402.
13. Huang CT, Sharma D, Oma P, Krishnamurthy R. Quantitation of protein particles in parenteral solutions using micro-flow imaging. *J Pharm Sci*. 2009;98:3058-3071.
14. Sharma DK, King D, Oma P, Merchant C. Micro-flow imaging: flow microscopy applied to sub-visible particulate analysis in protein formulations. *AAPS J*. 2010;12:455-464.
15. Sharma DK, Oma P, Pollo MJ, Sukumar M. Quantification and characterization of subvisible proteinaceous particles in opalescent mAb formulations using micro-flow imaging. *J Pharm Sci*. 2010;99:2628-2642.
16. Strehl R, Rombach-Riegraf V, Diez M, et al. Discrimination between silicone oil droplets and protein aggregates in biopharmaceuticals: a novel multiparametric image filter for sub-visible particles in microflow imaging analysis. *Pharm Res*. 2012;29:594-602.
17. Demeule B, Messick S, Shire SJ, Liu J. Characterization of particles in protein solutions: reaching the limits of current technologies. *AAPS J*. 2010;12:708-715.
18. Zolls S, Gregoritza M, Tantipolphan R, et al. How subvisible particles become invisible-relevance of the refractive index for protein particle analysis. *J Pharm Sci*. 2013;102:1434-1446.
19. Singh SK, Afonina N, Awwad M, et al. An industry perspective on the monitoring of subvisible particles as a quality attribute for protein therapeutics. *J Pharm Sci*. 2010;99:3302-3321.
20. Hyll K, Farahani F, Mattson L. *Doctoral Thesis: Optical Methods for Fines and Filler Size Characterization: Evaluation and Comparison. Inventia Reports*. 2016.
21. Erdbrugger U, Rudy CK, Etter ME, et al. Imaging flow cytometry elucidates limitations of microparticle analysis by conventional flow cytometry. *Cytometry A*. 2014;85:756-770.
22. Headland SE, Jones HR, D'Sa AS, Perretti M, Norling LV. Cutting-edge analysis of extracellular microparticles using ImageStream(X) imaging flow cytometry. *Sci Rep*. 2014;4:5237.
23. Ludwig DB, Trotter JT, Gabrielson JP, Carpenter JF, Randolph TW. Flow cytometry: a promising technique for the study of silicone oil-induced particulate formation in protein formulations. *Anal Biochem*. 2011;410:191-199.
24. Zolls S, Weinbuch D, Wiggenhorn M, et al. Flow imaging microscopy for protein particle analysis—a comparative evaluation of four different analytical instruments. *AAPS J*. 2013;15:1200-1211.
25. Hawe A, Sutter M, Jiskoot W. Extrinsic fluorescent dyes as tools for protein characterization. *Pharm Res*. 2008;25:1487-1499.
26. Demeule B, Gurny R, Arvinte T. Detection and characterization of protein aggregates by fluorescence microscopy. *Int J Pharm*. 2007;329:37-45.
27. Demeule B, Lawrence MJ, Drake AF, Gurny R, Arvinte T. Characterization of protein aggregation: the case of a therapeutic immunoglobulin. *Biochim Biophys Acta*. 2007;1774:146-153.
28. Mach H, Bhambhani A, Meyer BK, et al. The use of flow cytometry for the detection of subvisible particles in therapeutic protein formulations. *J Pharm Sci*. 2011;100:1671-1678.
29. Lin GL, Pathak JA, Kim DH, et al. Interfacial dilatational deformation accelerates particle formation in monoclonal antibody solutions. *Soft Matter*. 2016;12:3293-3302.
30. Ripple DC, Hu Z. Correcting the relative bias of light obscuration and flow imaging particle counters. *Pharm Res*. 2016;33:653-672.
31. Ripple DC, Montgomery CB, Hu Z. An interlaboratory comparison of sizing and counting of subvisible particles mimicking protein aggregates. *J Pharm Sci*. 2015;104:666-677.
32. Boivin S, Kozak S, Meijers R. Optimization of protein purification and characterization using Thermofluor screens. *Protein Expr Purif*. 2013;91:192-206.